FEMS Microbes, 2026, **7**, xtaf020
DOI: 10.1093/femsmc/xtaf020
Advance access publication date: 18 December 2025
Research Article – Microbes & Disease

Linezolid and levofloxacin: an uncommon pairing that suppresses evolution of resistance in *E. faecalis*

Noah M. Schlachter[1,5], Keanu Guardiola Flores[1], Kevin B. Wood[1,2,‡], Jeff Maltas[3,4,*]

[1]Department of Biophysics, University of Michigan, Ann Arbor, MI 48109, United States
[2]Department of Physics, University of Michigan, Ann Arbor, MI 48109, United States
[3]Department of Biology, University of Maryland, College Park, MD 20740, United States
[4]Department of Physics, University of Maryland, College Park, MD 20740, United States
[5]Present address: Department of Pharmacology, University of North Carolina, Chapel Hill, NC 27599, United States
*Corresponding E-mail: Department of Biology, 1204 Biology-Psychology Building, College Park, MD 20742-4415, United States. E-mail: jamaltas@umd.edu
Editor: Breck Duerkop
‡Deceased

Abstract

Drug combinations offer one potential strategy for slowing the evolution of antibiotic resistance. In this work, we investigate the evolution of drug resistance (strictly, the decrease in susceptibility) in populations of *Enterococcus faecalis*, an opportunistic human pathogen, exposed to different concentrations of the rarely used combination of linezolid (LZD) and levofloxacin (LEV). Using continuous culture bioreactors, we measured the two-dimensional dose–response surface of ancestral populations of *E. faecalis*, revealing that the LZD–LEV combination is strongly antagonistic, resulting in increased growth as LZD concentration is increased at a (sufficiently high) fixed concentration of LEV. Next, we performed multiday (50+ hour) evolution experiments by continually exposing populations to four different fixed-concentration combinations and then characterized isolates from adapted populations using whole genome sequencing and phenotypic dose–response curves. To control for differences in inhibition levels for different concentration combinations, we chose LZD–LEV combinations that fall along a single contour of constant growth in the two-drug space of LZD–LEV concentrations. Despite similar levels of initial inhibition across the four concentration combinations, we found that adaption is markedly different, with the most rapid adaptation and highest levels of evolved resistance occurring at combinations that include a high concentration of one drug and low concentration of the other. By contrast, we found almost no adaptation when both drugs were used at high concentrations, an initially surprising result that can be explained by simple drug-rescaling arguments applied to the antagonistic dose–response surface. Our results underscore the potential utility of a nonstandard (and strongly antagonistic) drug combination in suppressing resistance.

Keywords: antibiotic; resistance; drug combinations; *E. faecalis*; drug rescaling; evolution

Introduction

The rapid increase in antibiotic resistance presents a growing danger to public health (Davies and Davies 2010, Smith et al. 2015). Finding new antimicrobial treatments is a challenging and lengthy process, highlighting the urgency for innovative approaches that maximize the effectiveness of existing drugs. Combining drugs shows promise as a strategy to combat resistance, and considerable research has gone into identifying and predicting the effects of different drug combinations (Yeh et al. 2009, Baym et al. 2016, Beganovic et al. 2018). Traditionally, synergistic interactions, where combined drugs have a greater than additive effect, have been preferred for their potent antimicrobial effects at lower concentrations (Greco et al. 1995). However, a number of studies indicate that such synergy may actually hasten resistance evolution, while antagonistic interactions could slow or even reverse it (Chait et al. 2007, Hegreness et al. 2008, Michel et al. 2008, Palmer and Kishony 2013, Dean et al. 2020, Gjini and Wood 2021). This picture is further complicated by the potential for collateral effects, where resistance to one drug is associated with increased resistance or sensitivity to a second drug (Imamovic and Sommer 2013, Imamovic et al. 2018, Huynh et al. 2023, Maltas et al. 2020, 2025, Pál et al. 2015, Maltas and Wood 2019, Nichol et al. 2019, Rosenkilde et al. 2019, Roemhild and Andersson 2021, Ardell and Kryazhimskiy 2021, Beardmore et al. 2017, Barbosa et al. 2018). In this work, we investigate the evolution of resistance in an opportunistic pathogen (*Enterococcus faecalis*) exposed to two commonly used antibiotics that are strongly antagonistic and therefore rarely, if ever, used in combination. Our results offer a laboratory case study of how judiciously chosen concentrations of antagonistic drugs pairs can impede the resistance that readily occurs when the drugs are used alone.

Multidrug resistance is often a concern in *Enterococcus* species, which are highly adaptable and frequently implicated in human infections (Gilmore and Clewell 2002, Arias et al. 2010, Clewell et al. 2014, Kristich et al. 2014, Miller et al. 2014, García-Solache and Rice 2019). For example, *E. faecalis* is associated with infective endocarditis, bacterial meningitis, and urinary tract infections, and vancomycin-resistant enterococci (VRE) accounted for nearly

Received 10 June 2024; **revised** 7 December 2025; **accepted** 8 December 2025

one-third of enterococcal infections, resulting in over 50 000 cases in hospitalized patients and over 5000 deaths in 2017 according to the CDC's 2019 Antibiotic Resistance Threats Report.

Linezolid (LZD) is an oxazolidinone antibiotic used in the first-line treatment of VRE infections. Resistance to LZD is frequently conferred by G2576T mutations in the 23S rRNA V domain. This resistance to LZD can be a serious clinical problem with limited therapeutic options (Bourgeois-Nicolaos et al. 2007, Kainer et al. 2007, Diaz et al. 2012, Yadav et al. 2017, Chen et al. 2018, Bai et al. 2019, Rodríguez-Noriega et al. 2020). Interactions between LZD and other drugs have been reported in the lab and, to a lesser degree, in clinical reports (Chen et al. 2020, Antonello et al. 2024). For example, synergy is observed between LZD and rifampicin *in vitro* and in some animal models (Chen et al. 2020). In contrast to previous studies focused on synergy, we hypothesized that combining LZD with an *antagonistic* drug partner may help to stave off the evolution of resistance to LZD, thus increasing the durability of response for this critical therapy. Antagonism has been previously demonstrated between LZD and fluoroquinolones in vancomycin-resistant strains of *E. faecalis* (Sweeney and Zurenko 2003). Therefore, we selected an example fluoroquinolone (levofloxacin) as a sample antagonistic drug partner to study in combination with LZD. Resistance to levofloxacin (LEV) is not uncommon in isolates of enterococci (see, for example Chatterjee et al. 2024), and we hypothesized that antagonism between the two drugs may reduce evolution of resistance to both drugs.

Specifically, in this work we investigate the evolution of drug resistance in *E. faecalis* populations exposed to different concentration combinations of LZD and LEV. By measuring real-time per capita growth rate using continuous culture bioreactors (Fig. 1), we first mapped out the two-dimensional dose–response surface of ancestral ("wild type" or WT) populations of *E. faecalis*. We found that the LZD–LEV combination is strongly antagonistic, with low concentrations of LZD suppressing the inhibitory effects of sufficiently high LEV concentrations, resulting in a regime of increased growth as LZD concentration is increased. Next, we performed multiday (50+ hour) evolution experiments by exposing populations to four different concentration combinations while monitoring per-capita growth over time. To control for differences in inhibition levels for different concentration combinations, we chose LZD–LEV combinations that fall along a single contour of constant growth in the two-drug space of LZD–LEV concentrations. Following laboratory evolution, we characterized isolates from adapted populations using whole genome sequencing and phenotypic dose–response curves. Despite similar levels of initial inhibition across the four concentration combinations, we found that evolutionary trajectories are markedly different, with the most rapid growth increase and highest levels of evolved resistance occurring at combinations that include a high concentration of one drug and low concentration of the other. By contrast, we found almost no growth increase when both drugs were used at high concentrations, an initially surprising result that can be explained by simple drug-rescaling arguments applied to the antagonistic dose–response surface. Our results underscore the potential utility of nonstandard (antagonistic) drug interactions in suppressing resistance, at least in controlled laboratory conditions.

A note on terminology is in order: in what follows we define resistance as a measurable decrease in susceptibility to a given drug, quantified by the half maximal inhibitory concentration (IC50), which can be precisely measured in the lab under the same conditions as the evolution experiments. We do not mean to imply that any particular clinical breakpoint has been met, but for convenience choose the term "resistance" over the cumbersome "decrease in susceptibility." In addition, because our primary measure of fitness is per capita growth rate, we refer to the increase in per capita growth rate of the population as "adaptation" and sometimes shorten "per capita growth rate" to simply "growth" or "growth rate."

Materials and methods

Strains, antibiotics, and media

All resistant lineages were derived from *E. faecalis* V583, a fully sequenced vancomycin-resistant clinical isolate. The antibiotics used include LZD (brand) and LEV 98.0+%, TCI America™. Each antibiotic was prepared from powder stock and stored at −20°C. All experiments were started from overnight cultures inoculated from single colonies grown on brain heart infusion (BHI) agar plates and incubated in sterile BHI media overnight at 37°C.

Continuous culture device

Experiments were performed using the eVolver continous culture device. Populations were grown in glass vials with 24.5 ml BHI and 500 µl of cells cultured overnight. Each vial contains input and output channels connected to peristaltic pumps via silicone tubing. The eVolver device regularly measures cell density via emitter/detector LED pairs. When the eVolver detects cell density is too high, media/waste is pumped out of the vial. In order to keep the volume and drug concentration constant, an equal volume of fresh media with the same drug concentration is pumped into the vial. Cell density was measured at 10 s intervals in each vial using emitter/detector pairs of infrared LEDs.

Measuring drug combination effects in microplates

Preliminary screens to probe for drug interactions, specifically antagonism, utilized 96-well plate growth assays in which increasing concentrations of LZD were aliquoted along the columns of the plate and increasing concentrations of LEV were aliquoted along the rows, with the first column containing only LZD and the first row containing only LEV. Overnight cultures were diluted 40X into each well and cells were allowed to grow for 8 h before optical density was measured using a 96-well plate reader.

Measuring drug combination effects in bioreactor

Precise measurements of the LZD/LEV response surface were conducted in computer controlled bioreactors ["eVOLVER" from FynchBio, originally developed in Wong et al. (2018)]. The bioreactor was set to maintain constant cell density ("turbidostat mode") using a simple control algorithm that supplies fresh media/drug and removes cells when optical density has eclipsed the desired threshold. Per capita growth rate was then calculated from the pump rate required to maintain constant density; specifically, the pump flow rate for each pump was set to a constant value and pumping was turned on or off in real time. Growth was estimated from the pump log data as the fraction of time the pumps were "on" during the experiment and normalized by the same measurement in untreated cells.

Laboratory evolution experiments

Evolution experiments to combinations of differing concentrations of LZD and LEV were performed using the eVOLVER(Wong et al. 2018). Each condition was tested in duplicate using two aliquots from the same overnight culture, and evolution experiments lasted ∼60–80 h (though in several cases of rapid adaptation—for

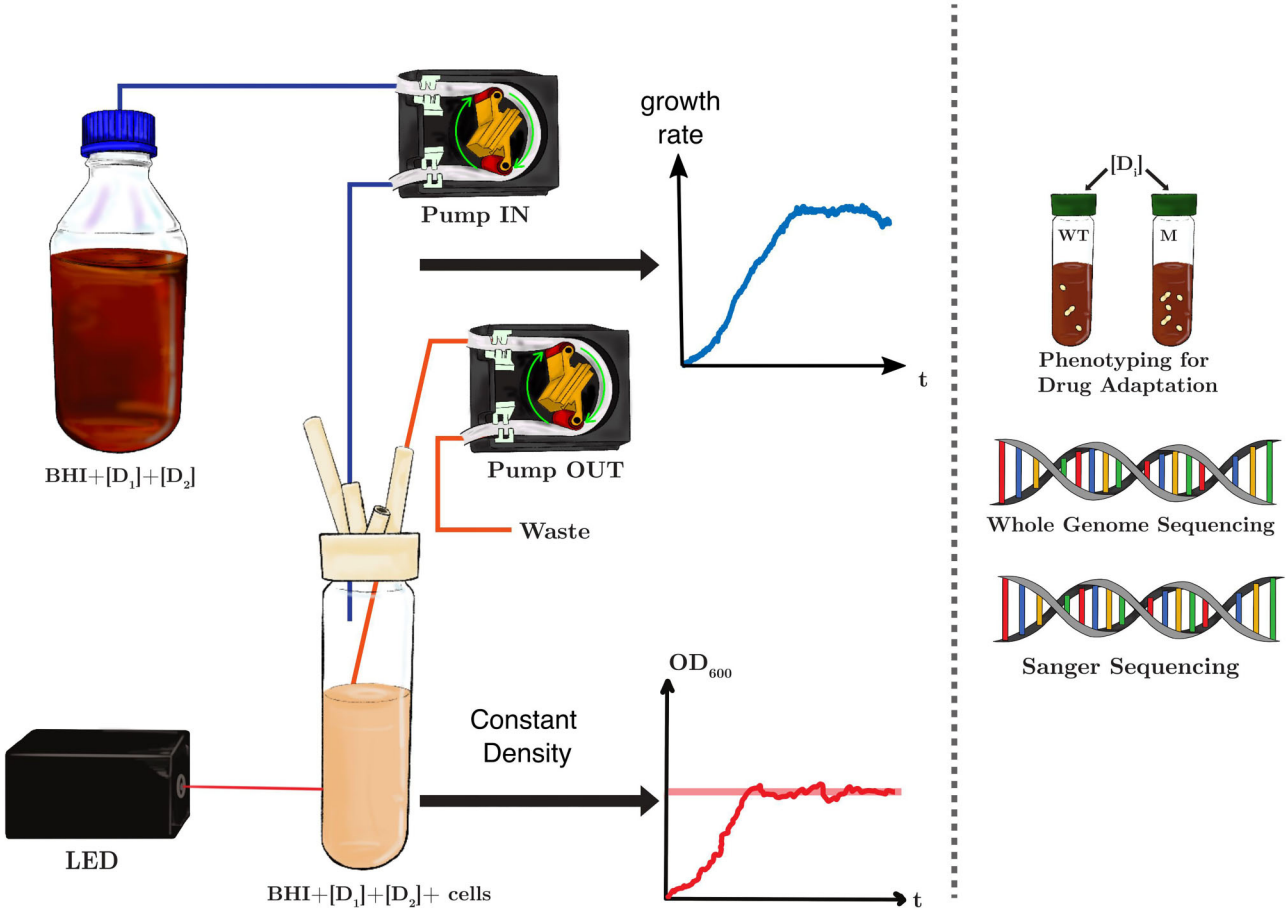

Figure 1. Measuring per capita growth rate (adaptation) in constant density bioreactors. Populations of *E. faecalis* are grown in $\mathbf{V} = 25$ ml cultures starting from $\sim 10^8$ cells of an overnight culture inoculated from a single colony of ancestral strain V583 (which we refer to as "wild type"). Population size is estimated using light scattering (OD) and held constant ("turbidostat mode") in exponential growth phase (OD ~0.2) using feedback control and peristaltic pumps, which provide fresh media and drug at the required rate. Growth rate $\mathbf{g}$ is estimated from the average flow rate of the pumps $\mathbf{F}(\mathbf{t})$ according to $\mathbf{g}(\mathbf{t}) = \frac{\mathbf{F}(\mathbf{t})}{\mathbf{V}}$. (In practice, pump flow rates are set to a fixed value but switched on or off according to the OD reading; $\mathbf{F}(\mathbf{t})$ is therefore estimated using the fraction of time a given pump is in the "on" state during sliding windows of ~10 min). All growth rates are normalized by growth of ancestral cells in the absence of drug ($\mathbf{g}_0 \approx 1/\mathrm{h}$). Populations were allowed to adapt to constant drug concentrations for a total of ~60 h, after which samples were taken for phenotyping and sequencing.

example, conditions A and B of Fig. 2—we stopped the evolution experiments when the media/drug reservoirs ran out of media). Following the evolution experiments, samples from all populations were stocked in 30% glycerol for storage at −80°C. Strains were also plated on pure BHI plates, and three colonies from each plate were selected for phenotyping (IC50 determination).

Measuring drug resistance and sensitivity

Experiments to estimate IC50 were conducted using 96-well plate assays performed in triplicate by exposing mutants and wild-type cells to increasing concentrations of only LZD and only LEV. Cells were cultured overnight in BHI. 5 µl cells were added to each well along with 195 µl of BHI. Cells were then allowed to grow and optical density at 600 nm was measured at 8 and 12 h using an Enspire Multimodal Plate Reader (Perkin Elmer) with an automated 20-plate stacker assembly. The OD (OD600) measurements for each drug concentration were normalized by the OD600 in the absence of drug. To quantify drug resistance, the resulting dose–response curve was fit to a Hill-like function $f(x) = (1 + (x/K)^h)^{-1}$ using nonlinear least squares fitting (MATLAB's nlinfit). K is the IC50 and h is a Hill coefficient describing the steepness of the dose–response relationship. The degree of resistance acquired to a drug after evolution is calculated as the fold-change in IC50 measured in evolved cells relative to an ancestral population. To determine if differences in observed IC50s between conditions were statistically significant we performed an F-test where the IC50 of the Hill function was allowed to vary between statistical groups. An F-test P-value ($P < .05$) indicates there is a statistical difference between the IC50 values between groups.

Genome extractions

Frozen samples of each mutant where grown at 37°C in sterile REMEL™ BHI Broth-Brain Heart Infusion (37 g in 1 l demineralized water) for 24 h. Genomic DNA from each overnight was then extracted using the Thermo Scientific GeneJET™ Genomic DNA purification kit, following their Gram-positive bacteria genomic DNA purification protocol.

PCR amplifications

Each one of the four copies of the 23S rRNA gene from each mutant's genome was polymerase chain reaction (PCR) amplified using Thermo Scientific™ Phusion™ Plus PCR Master Mix. Thermal cycler parameters for copies I, II, and IV of the 23S rRNA gene were chosen from the suggested three-step protocol provided with

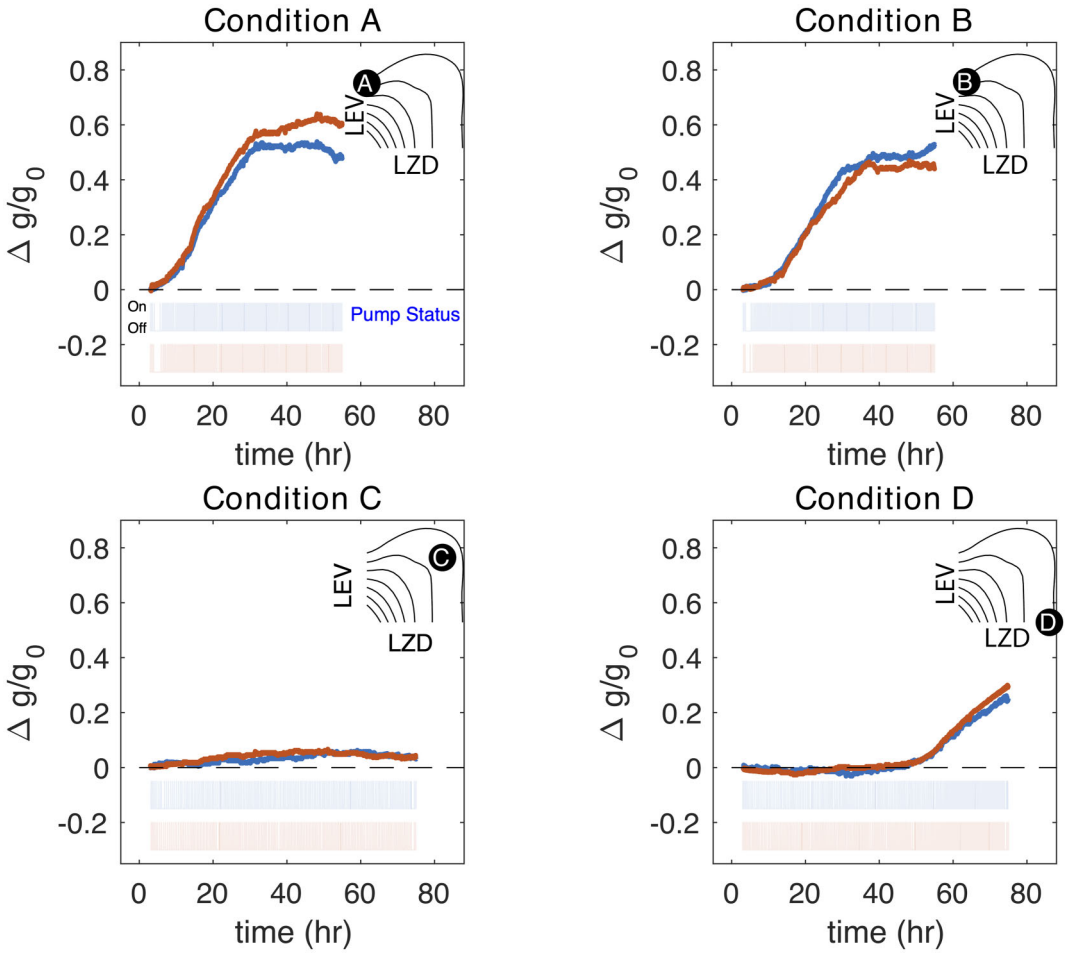

Figure 2. Rate of evolutionary adaptation depends on specific concentrations of LZD and LEV. Increase in per capita growth rate **Δg** (normalized by growth rate in absence of drug, $\mathbf{g}_0$) for ancestral populations of *E. faecalis* exposed to different concentrations of LEV and LZD. Red and blue curves represent two replicate populations; each inoculated from the same overnight culture. Lower insets show the status of the refresh pumps ("on" vs. "off") for each population where the "off" state is indicated by white space. Upper insets show the location in LEV–LZD concentration space (represented as constant-growth contours) at which the adaptation takes place. All conditions correspond to an initial growth inhibition of ∼70% (see also Fig. 3).

the mix. For copy III, the annealing temperature was decreased to 50°C instead of the suggested 60°C to better match the annealing temperature of the primer.

Sanger sequencing

After PCR amplification of the 23S regions, PCR products were sent to Eurofins for Sanger sequencing of the domain V region, which is associated with *in vitro* LZD resistance (Bourgeois-Nicolaos et al. 2007). We were particularly interested in the canonical G2576T mutation associated with increased LZD resistance.

Whole-genome sequencing

We sequenced a single individual colony from each of the final populations in the experiment of Fig. 2. Illumina Short Read sequencing (400 Mbp/2.7 million reads) and DNA isolation were performed by the Microbial Genome Sequencing Center (MiGS) at the University of Pittsburgh.

The resulting genomic data was analysed using the high-throughput computational pipeline breseq (Barrick et al. 2014), with default settings. Genomes were aligned to *E. faecalis* strain V583 (accession numbers: AE016830–AE016833) after annotating the reference sequence for IS elements using ISEscan (Xie and Tang 2017). We removed from the subsequent analysis any variant that occurred in the ancestral V583 strain or that corresponded to a synonymous mutation.

Results

LZD suppresses the inhibitory effects of LEV, leading to a strong antagonistic interaction

Before investigating evolutionary adaptation to LEV and LZD, we first characterized the growth response of *E. faecalis* ancestral populations to LEV and LZD at different concentrations on short (≈ 5 h) timescales. To do so, we inoculated 25 ml BHI with overnight cultures of strain V583 and grew populations in computer-controlled bioreactors at a range of fixed drug concentrations for ∼5 h. To estimate population growth rate, we used a simple feedback algorithm to hold cell density constant (i.e. a turbidostat; Fig. 1); we then estimated per capita growth rate from the effective flow rate required to maintain that constant density. To construct a 2D growth response surface between LZD and LEV of sufficient resolution, we repeated this procedure for ∼40 nonuniformly spaced concentration combinations and averaged growth rate over an ∼4-h period following drug exposure at each concentration combination (Fig. 3).

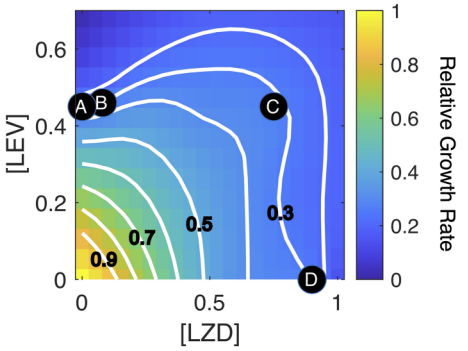

Figure 3. LZD and LEV interact antagonistically in *E. faecalis*. Per capita growth rate (normalized by growth in absence of drug) for ancestral populations of *E. faecalis* exposed to different concentrations of LEV and LZD. White curves are contours of constant growth (isoboles) in the 2D space of drug concentrations (measured in μg/ml). Black circles labeled A–D represent concentration combinations for adaptation experiments, all of which fall along the contour representing 70% growth inhibition. Growth surface was estimated using smoothing interpolation using measurements from ~40 nonuniformly spaced concentration combinations.

The LEV–LZD growth surface indicates that the two drugs interact antagonistically, with contours of constant growth ("isoboles") characterized by concave nonlinear shapes indicative of (Loewe; Greco et al. 1995) antagonism (Fig. 3). To illustrate the strong antagonism, consider increasing the concentration of LZD at a fixed LEV concentration of ~0.5 μg/ml. In the absence of LZD, growth is substantially inhibited, with growth rate ~20% of the drug-free rate (dark blue). However, as LZD is increased, growth initially increases (shading goes from dark blue to lighter blue), crossing several isoboles of constant growth before eventually declining again for concentrations of LZD above ~0.5 μg/ml. In words, at sufficiently high concentrations of LEV, the addition of an otherwise inhibitory drug (LZD) counterintuitively leads to an increase in growth, a classic signature of a so-called suppressive interaction between the drugs. While the mechanism of this effect has not been investigated for these specific drugs in this species, previous work in *Escherichia coli* has shown that protein synthesis inhibitors frequently suppress the effects of DNA synthesis inhibitors by alleviating a nonoptimal ratio of RNA and DNA in the cell (Bollenbach et al. 2009).

Adaptation rate depends on specific concentration combinations even when initial inhibition is constant across conditions

To investigate the evolution of resistance to different concentrations of LEV and LZD, we focused on four different concentration combinations: two combinations (A and D) that involve only a single drug and two (B and C) that involve both drugs together. To ensure that the initial inhibitory effects of the different combinations were approximately the same, we chose concentration combinations (A–D) that all fall on the isobole of ~70% inhibition (Fig. 3). Here 70% is arbitrarily chosen, but represents a strong selection pressure likely to rapidly select for resistant populations.

For each concentration combination, we grew two replicate populations (each inoculated from the same overnight culture) with the appropriate drug concentrations at a constant density for more than 50 h. Following the addition of drug, we observed a long period of approximately constant growth rate followed by a rapid increase of growth in three of the conditions (six populations) (Fig. 2, conditions A, B, and D). Both the timing and the steepness of the growth increase depend on the condition, with the most rapid adaptation (with a steep rise at ~10 h) occurring in conditions A and B, which contain (relatively) high concentrations of LEV. By contrast, adaptation is considerably delayed in the presence of LZD (condition D), but growth begins to rapidly increase after ~50 h.

By contrast, there is very little increase in growth in condition C, which contains (relatively) high concentrations of both drugs (when used alone, these concentrations would result in greater than the chosen 70% inhibition threshold). We note that these populations continued to grow throughout the experiment, but their per capita growth remained near the initial value (~30% of the drug-free growth rate in ancestral cells). The lack of adaption is therefore not a result of extremely high levels of inhibition—something that might be expected if drugs were used at concentrations that exceed the so-called mutant selection window.

Interestingly, we also observed substantial increase in growth rate in a drug-free evolution experiment, with the per capita growth rate increasing by nearly 30% over 50 h (though it should be noted that the initial growth rate was considerably higher—about a factor of 3—in these drug-free cultures compared to the with-drug cultures, so this evolution corresponds to ~3X the number of generations). These drug-free evolved populations exhibited no change in LZD resistance but a slight decrease in resistance to LEV relative to the ancestral ("WT") strain (Fig. S1).

Different iso-inhibitory concentration combinations lead to different levels of resistance to component drugs

Following the adaptation phase, we measured dose–response curves for isolates from each of the adapted populations (Fig. 4). We found that isolates adapted under different conditions showed a range of different levels of resistance, as quantified by fold-changes in half-maximal inhibitor concentrations (IC50s), consistent with the wide divergence of growth adaptation trajectories. Populations adapted to conditions A and B—those with zero or small concentrations of LZD and higher concentrations of LEV—showed increased levels of LEV resistance ($P < 10^{-4}$, F-test) but no change in LZD resistance. On the other extreme, LZD-only adaptation (condition D) resulted in increased resistance to LZD ($P < 10^{-8}$, F-test) and little change in LEV resistance. Interestingly, however, isolates from condition C exhibited no increase in resistance to either drug. The lack of resistance is initially surprising, because condition C included high concentrations of both drugs. If the drugs did not interact, one would naively expect these concentrations to rapidly select for mutants to each drug—perhaps as a sequential series of stepwise increases in growth as resistance to each drug is acquired. Yet, there is little evidence of adaptation in growth rate or an increase in resistance levels.

Qualitatively similar trajectories are observed in an independent experiment

We repeated the experiment on a second day (albeit for a slightly shorter total time) and found qualitatively similar results, including rapid evolution of growth rate in conditions A and B, little to no adaptation in condition C, and (in this case) slight adaptation in condition D (Fig. S2). In addition, LEV resistance increased in only conditions A and B (Figure S3), while LZD resistance increased only in condition D (Fig. S4). In all cases, the two replicates from the same day (started from the same overnight) showed nearly identical trajectories—perhaps not surprisingly given the relatively large size of total population and the initial inoculum.

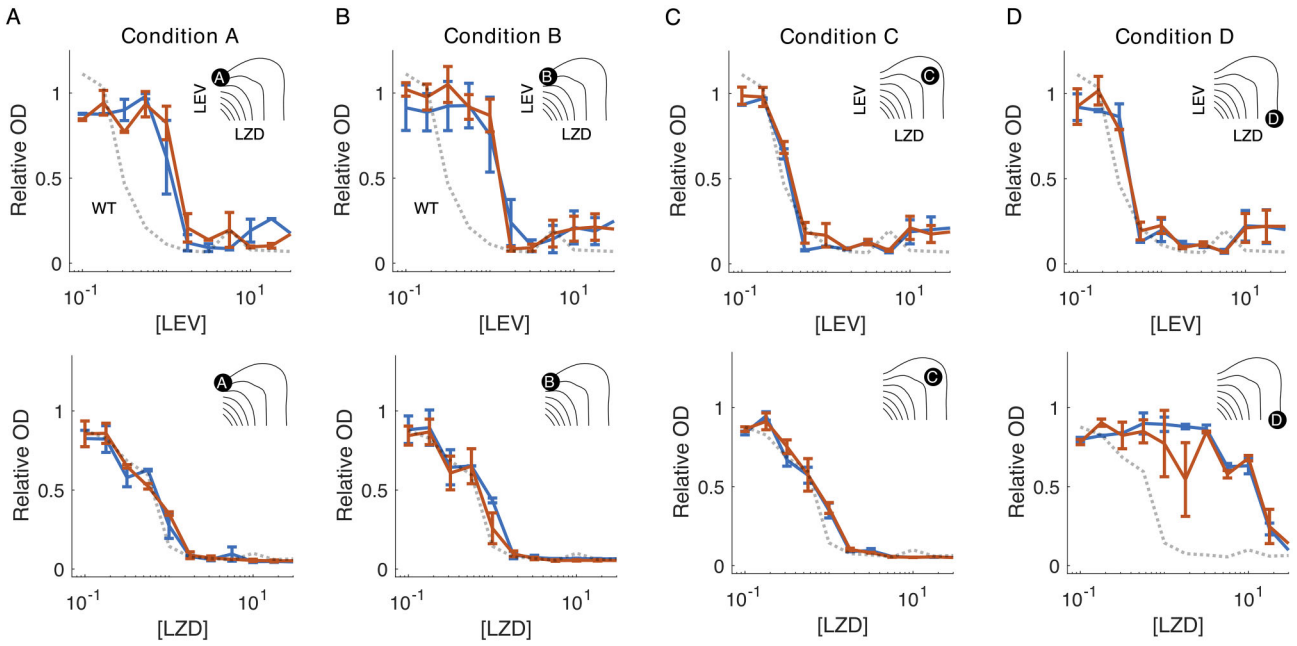

Figure 4. Resistance to component drugs depends on specific concentrations of LZD and LEV. Dose–response curves for individual isolates taken from two replicate adapted populations (blue and red), each inoculated from the same overnight culture. Top panels: LEV. Bottom panels: LZD. Dashed line is dos response curve for ancestral ("WT") population. Upper insets show the location in LEV–LZD concentration space (represented as constant-growth contours) at which the adaptation takes place. All concentrations are measured in units of μg/ml.

Whole genome sequencing reveals mutations in drug-specific targets

To further characterize the evolutionary process, we sequenced single colony isolates from each population (see the section "Methods"). Consistent with our phenotype measurements (Fig. 4), isolates evolved in conditions A and B all contained SNPs in *parC* (see Supplementary Information Data), a subunit of DNA topoisomerase IV and a well-known target of mutations conferring resistance to LEV and other quinolones (Yasufuku et al. 2011). Similarly, isolates from condition D (LZD-only) contained G2576T mutations (*E. coli* numbering) in multiple copies of the 23S rRNA V domain, a well-known source of LZD resistance (Bourgeois-Nicolaos et al. 2007). We confirmed these mutations via Sanger sequencing of the four distinct copies of the 23S rRNA gene (see the section "Methods"), revealing the G2576T mutation occurred in three copies in all isolates from condition D but did not occur in any other isolate. We identified several additional mutations in a single copy of 23S rRNA in isolates from other conditions, as well as a small number (between 0 and 5 mutations per isolate) of additional mutations in each isolate. But to our knowledge, these variants have not been previously associated with LZD or LEV resistance (see Tables S1–S3). As a whole, these results suggest that adaptation observed in conditions A, B, and D is due to selection for variants with increased resistance to one or both drugs and mutations in genes well-known to modulate resistance to LEV and/or LZD. These variants did not appear in isolates from condition C.

Drug-concentration rescaling arguments suggest LEV–LZD antagonism suppresses selection for resistance

It is initially surprising that growth adaptation occurred in both single-drug conditions (along with increases in resistance to one or both drugs and well-known resistance-conferring mutations) but did not occur when the drugs were used together. One hypothesis is that the resistant isolates could not arise in the presence of both drugs because of strong collateral sensitivity—that is, resistance to one drug is accompanied by an unwanted sensitivity to the other. However, this hypothesis is inconsistent with phenotype measurements (Fig. 4), which confirm that isolates exhibiting resistance to one drug do not exhibit increased sensitivity to the other drug. A second hypothesis could be that to survive in the presence of both drugs, a mutant would require multiple mutations–for example, one mutation in 23S rRNA (for LZD resistance) and one in *parC*. Indeed, if the drugs acted independently, one might expect growth adaptation curves to show multiple plateaus—first from acquisition of *parC* mutations and then, on that background, additional adaptation due to the acquisition of 23S rRNA mutations (or in the reverse order). Indeed, during adaptation to LEV alone we observe an increase in growth with a subsequent relative plateau (Fig. 2A). In a similar spirit, adaptation to LZD alone resulted in increases to growth, but the experiment ended before a plateau was reached (Fig. 2D). The absence of these sequential adaptations at condition C could suggest a strong epistasis between these mutations, but in that case, one would still expect to see one (or the other) mutation appear during the adaptation in condition C, though epistasis may preclude spread of a double mutant.

So why has the concentration combination in condition C suppressed the evolution of resistance? One explanation is given by simple drug rescaling arguments. These arguments, which were originally introduced in (Chait et al. 2007) and have since been formalized in (Chevereau et al. 2015, Das et al. 2020, Dean et al. 2020, Gjini and Wood 2021) and used in a number of nonevolutionary contexts (see, for example Wood and Cluzel 2012, Wood et al. 2014), are built on the assumption that populations of drug-resistant mutants respond to drug in a manner that is mathematically identical to drug-sensitive cells, as long as the true drug concentration is rescaled to a lower "effective" concentration. As a re-

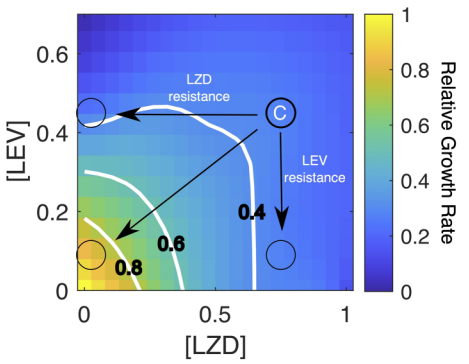

Figure 5. Rescaling of drug concentrations suggests single drug mutations are not advantageous at condition C. At the concentration combination at position C, a rescaling of only LEV concentration (e.g. due to mutations in parC; vertical black arrow) or only LZD concentration (e.g. due to mutations in 23S rRNA; horizontal black arrow) are not expected to dramatically change the growth rate. However, a simultaneous double mutation conferring resistance to both (diagonal arrow) would substantially increase growth rate. Open circles indicate the rescaled drug concentration, and therefore the growth rate, experienced by different mutants under drug rescaling assumptions. Drug response surface is the same as in Fig. 3.

sult, the dose–response surface measured in drug-sensitive cells (similar to Fig. 3) implicitly contains information about how resistant mutants will respond to the different drug combinations.

In our experiments, we observe two primary classes of mutants. Class 1 is resistant to only LEV, with mutants inhibited by LEV concentrations ~5 folder higher than ancestral cells (Fig. 4, panels A and B). Class 2 is resistant only to LZD, with mutants inhibited by LZD concentrations ~20–30 folder higher than ancestral cells (Fig. 4, panel D). How would these mutations—which correspond to decreases in LEV concentrations by a factor of 5 and decreases in LZD concentrations by a factor of 20–30—be expected to impact growth? It will depend on the condition. From Fig. 3, we can see that class 1 mutations would be expected to dramatically increase growth at conditions A and B (i.e. growth at the same LZD concentration but a 3–4 fold reduction in LEV at conditions A and B lead to almost completely restored growth that falls in the bright yellow region near the origin). By contrast, class I mutations would have little effect at positions C and D—moving directly downward from the points does not lead to a significant change in growth. By contrast, class II mutations would have little impact on growth at positions A, B, and C, where moving left along the LZD axis does not appreciably change growth, but would have a large effect at position D, leading to a substantial increase in growth. These rescaling arguments therefore suggest that mutations in class I and II, in isolation, would only be beneficial for populations under conditions A, B, and D, which is completely consistent with our experimental findings. These mutations, alone, would have little effect under condition C (Fig. 5). Intuitively, the lack of adaptation at position C occurs because of the strong antagonism between the drugs. For example, since LZD acts to suppress the effects of LEV, mutations in class II, that minimize the effects of LZD, therefore come with a hidden drawback–they also eliminate the benefit conferred by LZD in the presence of high levels of LEV.

Discussion

Our results complement a number of studies showing that interactions between drugs can modulate the rate at which resistance develops (Chait et al. 2007, Hegreness et al. 2008, Michel et al. 2008, Yeh et al. 2009, Dean et al. 2020, Gjini and Wood 2021). By performing evolution experiments in computer-controlled bioreactors, we were able to quantify growth-rate in real time over the course of the experiment, offering a detailed look at adaptation dynamics.

It is important to keep in mind several limitations of this work. Most importantly, these experiments are performed in a highly controlled *in vitro* environment, where complicating factors such as a patient's immune system, spatial drug gradients, and drug toxicity are all ignored. As such, these results alone cannot be directly applied to any given clinical situation. In addition, the concentrations used are sub-MIC concentrations, which allows the cells to grow, albeit slowly, throughout the course of the experiment. While scaling arguments (Gjini and Wood 2021) suggest similar qualitative behavior may occur at higher concentrations, these dynamics would need to be confirmed empirically by replicating these experiments at concentrations above the MIC. From a technical perspective, we have not attempted to quantify population heterogeneity within the evolving populations, though the similarity of the two replicates from each day suggests that the experiments are operating in a limit of large effective population size and are relatively deterministic. In addition, we focused on observed mutations with a known connection to LEV or LZD resistance, but additional variants are present in the fully sequenced data (Supplementary Information Data). While the observed mutations in *parC* and 23 s rRNA are consistent with the observed decrease in susceptibility to LEV and LZD, respectively, we can not rule out effects of other genetic changes or potential epistasis between variants. For example, while the breseq pipeline is able to predict many types of structural variants, it would likely not capture large scale IS-mediated changes that can occur in enterococci under stress, though recently developed sequencing technologies could be used to investigate these changes more thoroughly (Kirsch et al. 2023, Kirsch et al. 2024).

In addition, we focused on a single bacterial species, and all experiments were performed with the ancestral V583 *E. faecalis* strain. These results compliment several studies including those in *E. coli* (Yeh et al. 2009) and *S. aureus* (Lázár et al. 2022) where antagonistic drug combinations slow adaptation in these model systems. Still, it remains to be seen how repeatable these effects are in a more systematic study across diverse strains and species of bacteria. In addition to extending these results across diverse strains and species of bacteria, it would also be valuable to repeat this experiment with an assortment of fluroquinolones to ensure the result is general.

While we saw no evolved resistance for populations grown at high concentrations of both drugs (condition C), it is interesting to note that rescaling arguments suggest that low-level resistance to LZD could actually be favored under these conditions. Intuitively, LZD resistance corresponds to a rescaling of LZD concentration (Fig. 5), and LZD resistance at the levels we observed under other conditions (e.g. LZD alone, condition D) means the LZD rescaling would not appreciably increase growth rate. However, rescaling by a smaller factor—corresponding to a lower level of LZD resistance—is predicted to slightly increase growth rate as the rescaled point moves from location C leftward, to higher growth regions of drug–drug space, before eventually shifting to lower growth again as LZD resistance increases further. This suggests that low-level LZD-resistant mutants—perhaps those corresponding to 23S mutations in only a single copy of the gene (Bourgeois-Nicolaos et al. 2007)—might arise if the experiment is run for sufficiently long periods as to select for small fitness increases.

In general, antagonistic drug pairs are rarely chosen for clinical practice, in part because achieving a desired level of inhibition will require higher concentrations of one or both drugs, and in part because there is a drug-development focus on synergistic or noninteracting drug pairs. However, the results presented herein suggest that antagonistic drug combinations may play a future role as a valuable tool in a clinician's arsenal to slow the evolution of resistance, perhaps in chronic infections. Critically, before that step is taken, there remains important research to be done. For example, how does the role of the host immune system alter the selection pressure of the two-drug dose–response surface? How does the genetic background of the strain, its mutation rate, or horizontal gene transfer affect the adaptation rate? While much work remains to ensure care is not compromised for any individual patients, antagonistic drug combinations present a compelling avenue to slow evolution of resistance.

Acknowledgments

The authors would like to thank Brandon Wong and Ahmad Khalil for help troubleshooting the original eVOLVER setup.

Supplementary data

Supplementary data is available at FEMSMC online.

Conflict of interest: None declared.

Funding

This work was supported by the National Institutes of Health (NIH number 1R35GM124875 to K.B.W.).

References

Antonello RM, Riccardi N, Saderi L *et al.* Synergistic properties of linezolid against *Enterococcus* spp. isolates: a systematic review from in vitro studies. *Eur J Clin Microbiol Infect Dis* 2024;**43**:17–31. https://doi.org/10.1007/s10096-023-04704-8

Ardell SM, Kryazhimskiy S. The population genetics of collateral resistance and sensitivity. *eLife* 2021;**10**: e73250. https://doi.org/10.7554/eLife.73250.

Arias CA, Contreras GA, Murray BE. Management of multidrug-resistant enterococcal infections. *Clin Microbiol Infect* 2010;**16**:555–62. https://doi.org/10.1111/j.1469-0691.2010.03214.x

Bai B, Hu K, Zeng J *et al.* Linezolid consumption facilitates the development of linezolid resistance in *Enterococcus faecalis* in a tertiary-care hospital: a 5-year surveillance study. *Microb Drug Resist* 2019;**25**:791–8. https://doi.org/10.1089/mdr.2018.0005.

Barbosa C, Beardmore R, Schulenburg H *et al.* Antibiotic combination efficacy (ACE) networks for a *Pseudomonas aeruginosa* model. *PLoS Biol* 2018;**16**:e2004356. https://doi.org/10.1371/journal.pbio.2004356

Barrick JE, Colburn G, Deatherage DE *et al.* Identifying structural variation in haploid microbial genomes from short-read resequencing data using breseq. *BMC Genomics* 2014;**15**:1–17. https://doi.org/10.1186/1471-2164-15-1039

Baym M, Stone LK, Kishony R. Multidrug evolutionary strategies to reverse antibiotic resistance. *Science* 2016;**351**:aad3292. https://doi.org/10.1126/science.aad3292.

Beardmore RE, Peña-Miller R, Gori F *et al.* Antibiotic cycling and antibiotic mixing: which one best mitigates antibiotic resistance?. *Mol Biol Evol* 2017;**34**:802–17.

Beganovic M, Luther MK, Rice LB *et al.* A review of combination antimicrobial therapy for *Enterococcus faecalis* bloodstream infections and infective endocarditis. *Clin Infect Dis* 2018;**67**:303–9. https://doi.org/10.1093/cid/ciy064.

Bollenbach T, Quan S, Chait R *et al.* Nonoptimal microbial response to antibiotics underlies suppressive drug interactions. *Cell* 2009;**139**:707–18. https://doi.org/10.1016/j.cell.2009.10.025

Bourgeois-Nicolaos N, Massias L, Couson B *et al.* Dose dependence of emergence of resistance to linezolid in *Enterococcus faecalis in vivo*. *J Infect Dis* 2007;**195**:1480–8. https://doi.org/10.1086/513876

Chait R, Craney A, Kishony R. Antibiotic interactions that select against resistance. *Nature* 2007;**446**:668–71. https://doi.org/10.1038/nature05685.

Chatterjee R, Chakraborty A, Biswas M *et al.* Clinico-microbiological profile on multidrug-resistant enterococci in urinary tract infection patients in a tertiary care hospital. *Environ Dis* 2024;**9**:23–28. https://doi.org/10.4103/ed.ed_18_23

Chen H, Du Y, Xia Q *et al.* Role of linezolid combination therapy for serious infections: review of the current evidence. *Eur J Clin Microbiol Infect Dis* 2020;**39**:1043–52. https://doi.org/10.1007/s10096-019-03801-x

Chen M, Pan H, Lou Y *et al.* Epidemiological characteristics and genetic structure of linezolid-resistant *Enterococcus faecalis*. *IDR* 2018;**11**: 2397–409. https://doi.org/10.2147/IDR.S181339

Chevereau G, Dravecká M, Batur T *et al.* Quantifying the determinants of evolutionary dynamics leading to drug resistance. *PLoS Biol* 2015;**13**:e1002299. https://doi.org/10.1371/journal.pbio.1002299

Clewell DB, Gilmore MS, Ike Y *et al. Enterococci: From Commensals to Leading Causes of Drug Resistant Infection*. Boston: Massachusetts Eye and Ear Infirmary, 2014.

Das SG, Direito SOL, Waclaw B *et al.* Predictable properties of fitness landscapes induced by adaptational tradeoffs. *eLife* 2020;**9**:e55155. https://doi.org/10.7554/eLife.55155.

Davies J, Davies D. Origins and evolution of antibiotic resistance. *Microbiol Mol Biol Rev* 2010;**74**:417–33. https://doi.org/10.1128/MMBR.00016-10

Dean Z, Maltas J, Wood KB. Antibiotic interactions shape short-term evolution of resistance in *E. faecalis*. *PLoS Pathog* 2020;**16**:e1008278. https://doi.org/10.1371/journal.ppat.1008278

Diaz L, Kiratisin P, Mendes RE *et al.* Transferable plasmid-mediated resistance to linezolid due to cfr in a human clinical isolate of *Enterococcus faecalis*. *Antimicrob Agents Chemother* 2012;**56**:3917–22. https://doi.org/10.1128/AAC.00419-12

García-Solache M, Rice LB. The *Enterococcus*: a model of adaptability to its environment. *Clin Microbiol Rev* 2019;**32**:10–1128

Gilmore MS, Clewell DB. *The enterococci: pathogenesis, molecular biology, and antibiotic resistance*. Washington: ASM Press, 2002. https://doi.org/10.1128/9781555817923.

Gjini E, Wood KB. Price equation captures the role of drug interactions and collateral effects in the evolution of multidrug resistance. *eLife* 2021;**10**:e64851. https://doi.org/10.7554/eLife.64851.

Greco WR, Bravo G, Parsons JC. The search for synergy: a critical review from a response surface perspective. *Pharmacol Rev* 1995;**47**:331–85. https://doi.org/10.1016/S0031-6997(25)06847-4.

Hegreness M, Shoresh N, Damian D *et al.* Accelerated evolution of resistance in multidrug environments. *Proc Natl Acad Sci USA* 2008;**105**:13977–81. https://doi.org/10.1073/pnas.0805965105

Huynh A, Maltas JA, Wood KB. Heterogeneous collateral effects in daptomycin-resistant *E. faecalis*. *bioRxiv* 2023:2023–12.

Imamovic L, Ellabaan MMH, Machado AMD *et al.* Drug-driven phenotypic convergence supports rational treatment strategies of

chronic infections. *Cell* 2018;**172**:121–134.e14. https://doi.org/10.1016/j.cell.2017.12.012.

Imamovic L, Sommer MOA. Use of collateral sensitivity networks to design drug cycling protocols that avoid resistance development. *Sci Transl Med* 2013;**5**:204ra132. https://doi.org/10.1126/scitranslmed.3006609

Kainer MA, Devasia RA, Jones TF *et al.* Response to emerging infection leading to outbreak of linezolid-resistant enterococci. *Emerg Infect Dis* 2007;**13**:1024–30. https://doi.org/10.3201/eid1307.070019

Kirsch JM, Ely S, Stellfox ME *et al.* Targeted IS-element sequencing uncovers transposition dynamics during selective pressure in enterococci. *PLoS Pathog* 2023;**19**:e1011424. https://doi.org/10.1371/journal.ppat.1011424

Kirsch JM, Hryckowian AJ, Duerkop BA. A metagenomics pipeline reveals insertion sequence-driven evolution of the microbiota. *Cell Host Microbe* 2024;**32**:739–754.e4. https://doi.org/10.1016/j.chom.2024.03.005

Kristich CJ, Rice LB, Arias CA. Enterococcal infection—treatment and antibiotic resistance. In: *Enterococci: From Commensals to Leading Causes of Drug Resistant Infection*. Boston: Massachusetts Eye and Ear Infirmary, 2014.

Lázár V, Snitser O, Barkan D *et al.* Antibiotic combinations reduce *Staphylococcus aureus* clearance. *Nature* 2022;**610**:540–6

Maltas J, Huynh A, Wood KB. Dynamic collateral sensitivity profiles highlight opportunities and challenges for optimizing antibiotic sequences. *PLoS Biol* 2025;**23**: e3002970. https://doi.org/10.1371/journal.pbio.3002970.

Maltas J, Krasnick B, Wood KB. Using selection by nonantibiotic stressors to sensitize bacteria to antibiotics. *Mol Biol Evol* 2020;**37**:1394–406. https://doi.org/10.1093/molbev/msz303.

Maltas J, Wood KB. Pervasive and diverse collateral sensitivity profiles inform optimal strategies to limit antibiotic resistance. *PLoS Biol* 2019;**17**:e3000515. https://doi.org/10.1371/journal.pbio.3000515

Michel J-B, Yeh PJ, Chait R *et al.* Drug interactions modulate the potential for evolution of resistance. *Proc Natl Acad Sci USA* 2008;**105**:14918–23. https://doi.org/10.1073/pnas.0800944105

Miller WR, Munita JM, Arias CA. Mechanisms of antibiotic resistance in enterococci. *Expert Rev Anti Infect Ther* 2014;**12**:1221–36. https://doi.org/10.1586/14787210.2014.956092.

Nichol D, Rutter J, Bryant C *et al.* Antibiotic collateral sensitivity is contingent on the repeatability of evolution. *Nat Commun* 2019;**10**:334. https://doi.org/10.1038/s41467-018-08098-6

Pál C, Papp B, Lázár V. Collateral sensitivity of antibiotic-resistant microbes. *Trends Microbiol* 2015;**23**:401–07

Palmer AC, Kishony R. Understanding, predicting and manipulating the genotypic evolution of antibiotic resistance. *Nat Rev Genet* 2013;**14**:243–8. https://doi.org/10.1038/nrg3351

Rodríguez-Noriega E, Hernández-Morfin N, Garza-Gonzalez E *et al.* Risk factors and outcome associated with the acquisition of linezolid-resistant *Enterococcus faecalis*. *J Glob Antimicrob Resist* 2020;**21**:405–9. https://doi.org/10.1016/j.jgar.2020.01.010

Roemhild R, Andersson DI. Mechanisms and therapeutic potential of collateral sensitivity to antibiotics. *PLoS Pathog* 2021;**17**:e1009172. https://doi.org/10.1371/journal.ppat.1009172

Rosenkilde CEH, Munck C, Porse A *et al.* Collateral sensitivity constrains resistance evolution of the CTX-M-15 β-lactamase. *Nat Commun* 2019;**10**:1–10. https://doi.org/10.1038/s41467-019-08529-y

Smith RA, M'ikanatha NM, Read AF. Antibiotic resistance: a primer and call to action. *Health Commun* 2015;**30**:309–14. https://doi.org/10.1080/10410236.2014.943634.

Sweeney MT, Zurenko GE. In vitro activities of linezolid combined with other antimicrobial agents against staphylococci, enterococci, pneumococci, and selected Gram-negative organisms. *Antimicrob Agents Chemother* 2003;**47**:1902–6. https://doi.org/10.1128/AAC.47.6.1902-1906.2003

Wong BG, Mancuso CP, Kiriakov S *et al.* Precise, automated control of conditions for high-throughput growth of yeast and bacteria with eVOLVER. *Nat Biotechnol* 2018;**36**:614–23. https://doi.org/10.1038/nbt.4151

Wood KB, Cluzel P. Trade-offs between drug toxicity and benefit in the multi-antibiotic resistance system underlie optimal growth of *E. coli*. *BMC Syst Biol* 2012;**6**:48. https://doi.org/10.1186/1752-0509-6-48

Wood KB, Wood KC, Nishida S *et al.* Uncovering scaling laws to infer multidrug response of resistant microbes and cancer cells. *Cell Rep* 2014;**6**:1073–84. https://doi.org/10.1016/j.celrep.2014.02.007.

Xie Z, Tang H. ISEScan: automated identification of insertion sequence elements in prokaryotic genomes. *Bioinformatics* 2017;**33**:3340–7. https://doi.org/10.1093/bioinformatics/btx433.

Yadav G, Thakuria B, Madan M *et al.* Linezolid and vancomycin resistant enterococci: a therapeutic problem. *J Clin Diagnos Res* 2017;**11**:GC07.

Yasufuku T, Shigemura K, Shirakawa T *et al.* Mechanisms of and risk factors for fluoroquinolone resistance in clinical *Enterococcus faecalis* isolates from patients with urinary tract infections. *J Clin Microbiol* 2011;**49**:3912–6. https://doi.org/10.1128/JCM.05549-11

Yeh PJ, Hegreness MJ, Presser Aiden A *et al.* Drug interactions and the evolution of antibiotic resistance. *Nat Rev Microbiol* 2009;**7**:460–6. https://doi.org/10.1038/nrmicro2133

Received 10 June 2024; **revised** 7 December 2025; **accepted** 8 December 2025